ChemComm

Accepted Manuscript

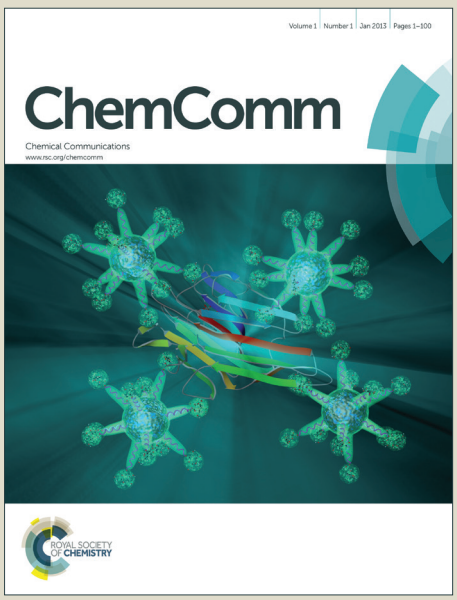




ROYAL SOCIETY OF CHEMISTRY

www.rsc.org/chemcomm

TOC

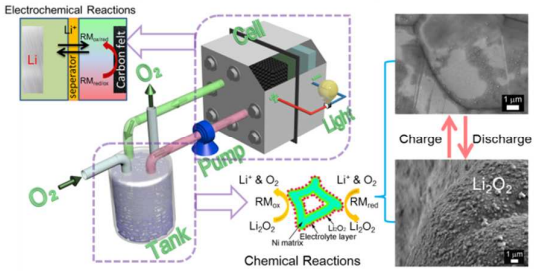


Redox-flow Li-$O_2$ battery addresses surface passivation and pore clogging problems of the cathode by using a pair of redox catalysts.

Journal Name RSCPublishing

COMMUNICATION

# Dual redox catalysts for oxygen reduction and evolution reactions: towards a redox flow Li-$O_2$ battery

Cite this: DOI: 10.1039/x0xx00000x

Yun Guang Zhu, Chuankun Jia, Jing Yang, Feng Pan, Qizhao Huang, Qing Wang*

Received 00th January 2015,
Accepted 00th January 2015

DOI: 10.1039/x0xx00000x

www.rsc.org/

**A redox flow lithium-oxygen battery (RFLOB) by using soluble redox catalysts with good performance was demonstrated for large-scale energy storage. The new device enables the reversible formation and decomposition of $Li_2O_2$ via redox targeting reactions in a gas diffusion tank, spatially separated from the electrode, which obviates the passivation and pore clogging of cathode.**

With the increasing demand for high-density energy storage, various electrochemical energy storage technologies have been proposed, of which lithium-oxygen (Li-$O_2$) battery is believed to be one of the most promising solutions.[1-5] Li-$O_2$ battery "breathes" oxygen from the air as reactant, which greatly enhances the gravimetric energy density and reduces the cost of the cell.[6] Therefore, Li-$O_2$ batteries have recently attracted considerable attention from all over the world. Despite the great promises, Li-$O_2$ battery confronts several critical issues before it becomes a credible solution for next generation energy storage, for instance, stability of aprotic electrolyte and electrode in the presence of $O_2^{\cdot-}$ radical, effectiveness of catalyst with the passivation of $Li_2O_2$, microstructures of cathode to accommodate $Li_2O_2$ while allow the access of $O_2$ and $Li^+$, and cyclability of lithium anode upon prolonged cycling, etc. While profound studies have been done in searching stable electrolytes[7-12] and efficient oxygen electrocatalysts[13-20], challenges relating to surface passivation and pore clogging by the insoluble $Li_2O_2$ in the gas diffusion cathode remain[21]. This severely impairs the round-trip energy efficiency and limits the achievable capacity of the cell. Recently, redox catalysis was introduced to mitigate the overpotentials for oxygen reduction or evolution reactions by utilizing redox mediators dissolved in the electrolyte.[22-29] These soluble redox active species could either reduce $O_2$ forming $Li_2O_2$ in the presence of $Li^+$ in the electrolyte, or oxidize $Li_2O_2$ releasing oxygen. Since the "catalysts" exist in the electrolyte, the adverse effect of surface passivation is alleviated. By contrast, these redox-catalyzed reactions towards $O_2$ in essence resemble the "redox targeting" reactions recently proposed for lithium-ion battery materials.[30-32] In the presence of suitable redox mediators in the electrolyte, battery materials could be charged and discharged through reversible chemical lithiation and delithiation without attaching to the current collector, which intuitively results in a novel battery system — redox flow lithium-ion batteries (RFLB). We notice a Li-air fuel cell system with circulating catholyte has been demonstrated by H. Zhou and co-workers.[33] The same group also proposed a flow system using soluble catalyst in an aqueous catholyte for the oxygen reduction reaction,[34] which in principle results of a redox flow Li-$O_2$ primary cell.

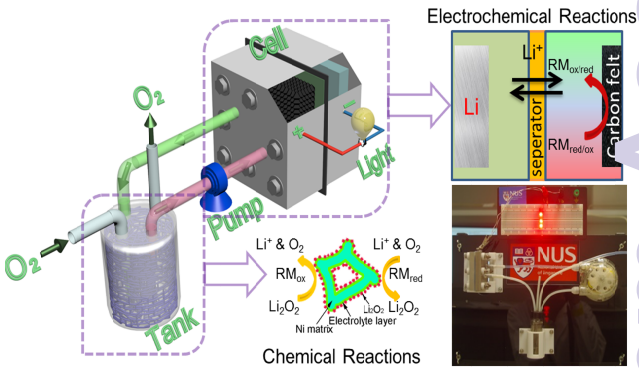


**Fig. 1.** Schematic illustrates the configuration and working process of a redox flow lithium-oxygen battery (RFLOB). The cell stack constitutes a lithium metal anode and carbon felt cathode (*2 cm × 2 cm*), separated by a membrane. A gas diffusion tank (GDT) is connected to the cathodic compartment through a pump. During discharge process, oxygen flows into the tank and is reduced to form $Li_2O_2$ while electrolyte fluid containing redox mediators and $Li^+$ circulates between GDT and cell. The photo at the lower right corner shows a RFLOB single cell powering three light-emitting diodes.

Here we demonstrate a new implementable solution — rechargeable redox flow Li-$O_2$ battery (RFLOB) to tackle the critical issues confronted by non-aqueous Li-$O_2$ batteries. As illustrated in Figure 1, the RFLOB has a gas diffusion tank (GDT) connected to the

electrochemical cell stack. Electrolyte fluid is circulated between the tank and cell by a peristaltic pump, in which for the first time we concurrently introduced two different redox mediators to catalyze the $O_2$ reduction and evolution reactions during discharging and charging processes, respectively. As a result, the use of conventional electrocatalysts on the cathode has been completely avoided. The GDT tank is filled with porous material allowing the easy access of redox fluid and $O_2$, in which the $O_2$ pressure is kept constant through a gas inlet and outlet. During discharging process, redox mediator $RM_1$ is reduced at cathode and flows into the GDT tank where it is oxidized by $O_2$ in the presence of $Li^+$:

$$RM_1^{ox} + e^- \rightarrow RM_1^{red} \text{ (electrochemical reaction on cathode)} \quad (1)$$

$$Li^+ + RM_1^{red} + O_2 \rightarrow Li_2O_2 + RM_1^{ox} \text{ (chemical reaction in GDT)} \quad (2)$$

In this process, $Li_2O_2$ is formed and deposited in the porous matrix of the GDT tank. The regenerated $RM_1$ then flows back to the cell for a second round of reactions. During charging process, another redox mediator $RM_2$ is oxidized at cathode and flows into the GDT tank where it is reduced by $Li_2O_2$ releasing $O_2$.

$$RM_2^{red} \rightarrow RM_2^{ox} + e^- \text{ (electrochemical reaction on cathode)} \quad (3)$$

$$Li_2O_2 + RM_2^{ox} \rightarrow Li^+ + RM_2^{red} + O_2 \text{ (chemical reaction in GDT)} \quad (4)$$

As the formation of $Li_2O_2$ occurs in the tank, surface passivation and pore clogging of the cathode are essentially avoided. In theory, the capacity of the cell would just be limited by the size of GDT tank should sufficient Li metal be used in the anodic compartment. In addition, as the redox mediators generally have fast reaction kinetics, low-cost carbon felt could be used as the cathodic current collector even without electrocatalyst, which is however indispensible in conventional Li-$O_2$ batteries. As such, a "catalyst-free" Li-$O_2$ battery could be developed, which is distinct from the conventional Li-$O_2$ cells. The redox potential of $Li_2O_2$ in aprotic solvent is ~2.96 V vs. $Li/Li^+$. Considering the redox potentials of ethyl viologen (EV) and iodide, which are ~2.65 V for $EV^+/EV^{2+}$ and ~3.10/3.70 V for $I^-/I_3^-/I_2$ (Figure 2a), just straddle that of $Li_2O_2$, these two redox species were identified as the mediators for oxygen reduction and evolution reactions in RFLOB, respectively. The potential difference between the mediators and $Li_2O_2$ provides the necessary thermodynamic driving force for the formation and decomposition of $Li_2O_2$ via redox targeting reactions[35], of which the lower potential of $EV^+$ enables the reduction of $O_2$ forming $Li_2O_2$ during discharge process (reaction 2), while the relatively positive potential of triiodide or iodine facilitates the oxidation $Li_2O_2$ during charge process (reaction 4). Both redox mediators have been tested in static cells and showed good reversibility (Figure S1).

As the photograph shown in Figure 1, RFLOB was fabricated with a GDT tank filled with 8 ml redox electrolyte consisting of 10 mM $EV^{2+}$/10 mM $I^-$ and 1.0 M lithium bis(trifluoromethane) sulfonimide (LiTFSI) in tetraethyleneglycol dimethylether (TEGDME). The $O_2$ pressure in the tank was kept at 1 *atm*. Vinylene carbonate pretreated lithium foil was used as anode in the electrochemical cell to preclude the reaction with redox mediators, since the Celgard® separator is unable to block the crossover of the redox mediators.[36, 37] The cell was discharged and charged in galvanostatic mode and the voltage profiles are shown in Figure 2b. In the first discharging process, only a single voltage plateau at ~2.70 V was observed, which matches the reduction of $EV^{2+}$. However, noting the theoretical discharge capacity of $EV^{2+}$ to $EV^+$ is only ~2 mAh, the much-extended capacity (here the cell capacity was controlled at 6 mAh) implies the reduction of $O_2$ by $EV^+$ in the GDT tank, forming $EV^{2+}$ and $Li_2O_2$ as revealed later. The regenerated $EV^{2+}$ then flows back to the cell and starts a second round of reduction meanwhile electricity is generated.

In theory, the above discharge process could carry on until Li metal in the anode is used up and reaches the theoretical specific energy of the cell. For instance, in a non-constrained discharge process close to 80% lithium was converted into $Li_2O_2$ with relatively low overpotential loss in the presence of 10 mM $EV^{2+}$ (Figure 2c), which paves a way of making low-cost and extremely high-energy density Li-$O_2$ primary cells.

During the charging process, two voltage steps appeared at ~3.55 and 3.75 V (Figure 2b). The oxidation of $EV^+$ was not observed since most of $EV^+$ have been oxidized to $EV^{2+}$ by the surplus $O_2$ in the tank. Hence the cell voltage shoots directly up to that for the oxidation of $I^-$ to $I_3^-$ upon charging, at which there seemed very limited reaction between $I_3^-$ and $Li_2O_2$ since the capacity extension at this voltage is rather small. Thereafter the voltage rises steadily until it reaches the second voltage plateau. Brown color was built up gradually in the electrolyte, indicating more and more polyiodide was produced. The high voltage plateau corresponds to the further oxidation of $I_3^-$ to higher order polyiodides and eventually to iodine. The extended capacity at the high voltage indicates the reaction between iodine and $Li_2O_2$ was efficient which resulted in the oxidation of the latter and releasing $O_2$.

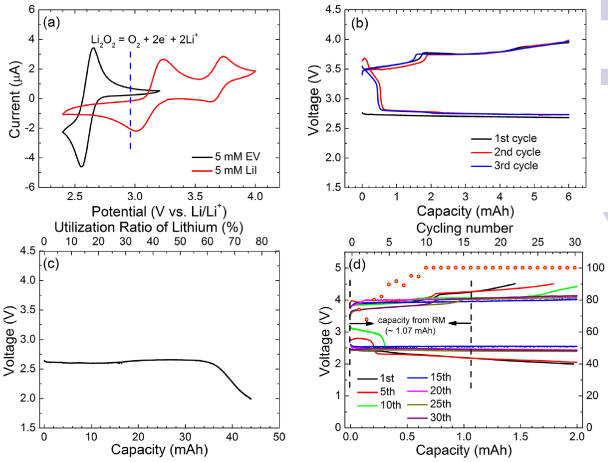


**Fig. 2.** (a) Cyclic voltammograms of EV and LiI in TEGDME. The scan rate is 0.10 V/s. The redox potential of $Li_2O_2$ is indicated for reference. (b) Discharge/charge curves of a RFLOB in the first 3 cycles. The current density is 0.05 mA/cm$^2$. (c) The discharge curve of a RFLOB primary cell showing the high utilization ratio of lithium anode in the presence of 10 mM $EV^{2+}$. The current density is 0.125 mA/cm$^2$. (d) Discharge/charge curves and Coulombic efficiency of a RFLOB employing a PVDF-Nafion membrane at different cycle numbers. The current density is 0.125 mA/cm$^2$. The electrolyte was 1.0 M LiTFSI in TEGDME containing10 mM $EV^{2+}$/10 mM $I^-$, with a volume of 8 ml in (b), (c), and 4 ml in (d).

The charge transfer process between $Li_2O_2$ and $I_2$ is corroborated by theoretical calculations. Figure S3 shows the electron density difference maps of $I_3^-$ and $I_2$ on $Li_2O_2$ (0001) surface in parallel adsorption geometry, where the blue and yellow zones correspond to electron density deduction and enhancement regions, respectively. Apparently there is a tendency of electron transfer from $Li_2O_2$ to both $I_3^-$ and $I_2$. The charge transfer is quantified by the Bader charge calculation to be 0.49 $e^-$ for $Li_2O_2/I_2$, relative to that for $Li_2O_2/I_3^-$, indicating much more effective electron transfer in the former as compared to the latter.

In the subsequent discharging process, a short voltage plateau appeared at ~3.30 V, attributed to the reduction of iodine in the electrolyte. After that, the cell voltage kept stable at ~2.70 V, exhibiting good reversibility of EV. In order to rule out the capacity

from the direct reduction of dissolved $O_2$ on the cathode, the cell was also tested in the absence of both redox mediators (Figure S2). It is obvious that given the extremely low capacity, the reaction of dissolved $O_2$ on the cathode has negligible contribution to the overall cell capacity. In general, one should note that these two molecules would not chemically react with each other upon operation. During discharging, both of the molecules will subsequently be reduced to $I^-$ and $EV^+$ in the cell. Similarly during charging, both of molecules will subsequently be oxidized to $EV^{2+}$ and $I_2$. So it is unlikely that both $I_2$ and $EV^+$ co-exist in the catholyte causing reaction between the two.

The above results are very encouraging that, since the deposition of $Li_2O_2$ mainly occurs in the GDT tank, which intrinsically obviates the passivation and pore clogging of cathode in the cell, very stable voltage profiles with relatively low overpotentials were achieved in the first three cycles, even in the absence of catalysts. To prove the formation and decomposition of $Li_2O_2$ in the GDT tank, X-ray photoelectron spectroscopy (XPS) was employed to investigate the chemical states of Li and O for species formed in the tank at the end of discharge and charge. The signal associated with Li-F bond (56.6 eV) presents in all the samples (Figure 3), presumably from the remained LiTFSI.[38] The peak of Li-O-O-Li (55.0 eV) is clearly seen in the Li 1s spectra after discharging while nearly disappeared after charging. The existence of $Li_2O_2$ is further corroborated by O 1s spectra, where two large peaks assigned to the O1s (532.3 eV) from LiTFSI and Li-O-O-Li (531.2 eV) in $Li_2O_2$ are evidently observed.[38, 39] The latter then vanished after charging, in agreement with the Li 1s spectra. In order to confirm the formation of $Li_2O_2$ on Ni foam in the GDT tank, XRD measurement was carried out with the sample after full discharging. As the diffraction pattern shown in Figure S4, the characteristic peaks of $Li_2O_2$ such as (101), (100) are clearly seen. These peaks are relatively broad in width in contrast to those from the Ni substrate, indicating the nanocrystalline nature of the formed $Li_2O_2$. In addition, some minor peaks, which may be assigned to LiOH and $Li_2CO_3$ phases, are also visible. These by-products may plausibly be introduced during sample transfer and/or XRD measurement, which were conducted in air. The XPS and XRD results were further substantiated by scanning and transmission electron microscopic measurements.

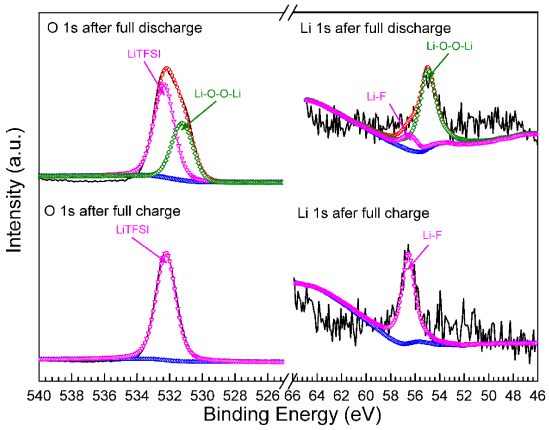


**Fig. 3.** X-ray photoemission spectroscopy (XPS) measurement of Li 1s and O 1s spectra and the corresponding peak deconvolutions. The upper and lower panels display those of the discharged and charged species in the GDT tank, respectively.

As the SEM images shown in Figure 4, after discharging the smooth surface of pristine Ni foam (Figure S5a) was covered by a layer of agglomerated particles (Figure 4a), which nearly disappeared with only little residual left after charging (Figure 4b). This is consistent with the XPS measurement should the particles be $Li_2O_2$. The cell in Figure 2c was also examined after full discharging, in which we expect much more product would be formed in the GDT tank. As revealed in Figure S5b, not surprisingly, a much thicker layer of particulate precipitate was observed on the Ni foam. The particles are in round shape and 10-20 nm in diameter (Figure 4c), which are crystalline in nature as revealed by the high resolution TEM. The lattice fringes of (101) and (100) crystal planes of $Li_2O_2$ are clearly identified (Figure 4d), with d-spacing of 0.25 nm and 0.27 nm respectively. This unambiguously confirms the formation of $Li_2O_2$ upon discharging.

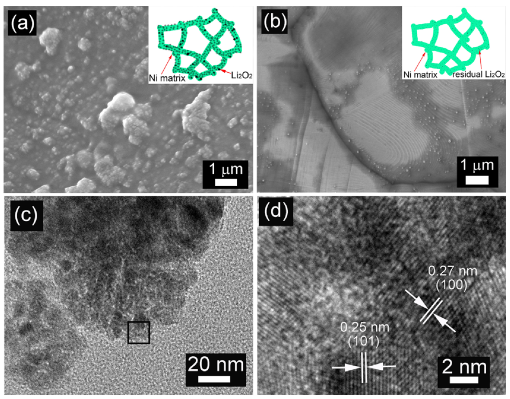


**Fig. 4.** (a-b) Field emission scanning electron microscopy (FESEM) images showing the morphology evolution of Ni foam after discharging (a) and re-charging (b) in the GDT tank. The insets illustrate the formation and decomposition of $Li_2O_2$ on the surface of Ni foam. (c-d) Transmission electron microscopy (TEM) and high-resolution TEM images showing the agglomerated nanoparticles (c) of $Li_2O_2$ and the lattice fringes (d).

The above results have convincingly validated the working principle of RFLOB. In order to assess the viability of the cell for long-term cycling, despite that it has yet been optimized and there are a few other critical issues to be addressed (such as the poor cyclability of lithium anode), we tested the cycling performance of the above RFLOB cell at a controlled discharging capacity ($Li_2O_2$ to redox molecules ratio is 1:1). A PVDF-Nafion composite membrane was employed to protect the lithium anode from being attacked by the redox mediators and dissolved $O_2$ upon repeated striping and plating in long cycling process. As the voltage profiles shown in Figure 2d, relatively large overpotential was observed due to the large IR drop across the membrane. Interestingly, with increasing cycle number, the overpotential of the cell decreased gradually, largely a result of the reduced resistance of the membrane over cycling. There isn't deterioration of charging capacity in the first 30 cycles. Instead, due to improved conductivity of the membrane, the charging capacity was even enhanced with the Coulombic efficiency reaching nearly 100% after 10th cycle (Figure 2d). As a preliminary proof-of-concept study, we do not attempt to study the influences of flow rate and other operation parameters on the overall device performance before the following factors are optimized: Firstly, the PVDF-Nafion membrane is resistive, which makes up a big IR drop. Secondly, the sluggish reaction between $I_2$ and $Li_2O_2$ and those of $I^-$ on the electrode account for a major loss of overpotential during charging. As a result, the discharging/charging current density is relatively low.

## Conclusions

The above results provide compelling evidence and concertedly validate the functionality of RFLOB. That is, with the assistance of redox mediators, the discharging product $Li_2O_2$ could be remotely formed in the GDT tank and reversibly oxidized in the charging

process without depositing onto the cathode inside the cell. Such decoupled reactions of $Li_2O_2$ provide great flexibility to circumvent the issues confronted by the conventional Li-$O_2$ batteries. The surface passivation and pore clogging of the cathode resulted from $Li_2O_2$ precipitations, which is inevitable in conventional cells, are essentially avoided under the new operation mode. While the overpotential persists during the charging process, the intolerably large voltage hysteresis could in theory be mitigated by using suitable redox mediators even in the absence of electrocatalysts, which on the other hand is expected to also improve the cycling stability of the cell. In addition, the capacity of the cathode could be expanded by simply enlarging the size of GDT tank, which is however constrained by the pore volume of cathode and catalysts deposited on it in the conventional Li-$O_2$ batteries. Moreover, as the reaction of $O_2$ in GDT is far apart from the electrodes, the tolerance of the cell towards air would be enhanced as well.

While promising, to develop RFLOB into a viable device for advanced large-scale energy storage, the large voltage hysteresis would have to be further reduced. In the present study, the stagnant reaction between triiodide and $Li_2O_2$ and resistive $Li^+$-conducting membrane represent the main causes of the large overpotential during charging process. Faster redox mediators with matched potential to the oxidation of $Li_2O_2$ are desired to expedite the reactions. In addition, optimization of the three-phase interface in the GDT tank to facilitate the reactions of $O_2$ and $Li^+$, and more effectively utilize the volume to accommodate $Li_2O_2$ is also required. Highly porous low-weight materials with good affinity to the deposition of $Li_2O_2$ and superior chemical resistance would be the ideal option. We are currently pursuing the above aspects to develop RFLOB into a low-cost and durable alternative to the Li-$O_2$ batteries for large-scale energy storage applications.

## Acknowledgments

This research was supported by the National Research Foundation, Prime Minister's Office, Singapore under its Competitive Research Programs (CRP Award No. NRF-CRP8-2011-04 and NRF-CRP10-2012-06).

## Notes and references

Department of Materials Science and Engineering, Faculty of Engineering, NUSNNI-NanoCore, National University of Singapore, 117576, Singapore.
*Correspondence to: E-mail: msewq@nus.edu.sg; Fax: +65 6776-3604; Tel: +65 6516-7118

†Electronic Supplementary Information (ESI) available: Materials and methods; Fig.S1-S4, CV curves of two redox molecules under various scan rates, the charge and discharge curves of RFLOB in the absence of redox mediators in the electrolyte, XRD and SEM micrograph of the formed $Li_2O_2$ in GDT tank. See DOI: 10.1039/c000000x/

1. E. L. Littauer and K. C. Tsai, *Journal of the Electrochemical Society*, 1976, **123**, 771-776.
2. E. L. Littauer and K. C. Tsai, *Journal of The Electrochemical Society*, 1977, **124**, 850-855.
3. K. Abraham and Z. Jiang, *Journal of The Electrochemical Society*, 1996, **143**, 1-5.
4. G. Girishkumar, B. McCloskey, A. Luntz, S. Swanson and W. Wilcke, *The Journal of Physical Chemistry Letters*, 2010, **1**, 2193-2203.
5. Y.-C. Lu, B. M. Gallant, D. G. Kwabi, J. R. Harding, R. R. Mitchell, M. S. Whittingham and Y. Shao-Horn, *Energy & Environmental Science*, 2013, **6**, 750-768.
6. N. Imanishi, A. C. Luntz and P. Bruce, Springer, 2014.
7. M. Bhatt, H. Geaney, M. Nolan and C. Odwyer, *Physical Chemistry Chemical Physics*, 2014, **16**, 12093-12130.
8. Y. Chen, S. A. Freunberger, Z. Peng, F. Bardé and P. G. Bruce, *Journal of the American Chemical Society*, 2012, **134**, 7952-7957.
9. Z. Peng, S. A. Freunberger, L. J. Hardwick, Y. Chen, V. Giordani, F. Bardé, P. Novák, D. Graham, J. M. Tarascon and P. G. Bruce, *Angewandte Chemie*, 2011, **123**, 6475-6479.
10. S. A. Freunberger, Y. Chen, Z. Peng, J. M. Griffin, L. J. Hardwick, F. Bardé, P. Novák and P. G. Bruce, *Journal of the American Chemical Society*, 2011, **133**, 8040-8047.
11. S. A. Freunberger, Y. Chen, N. E. Drewett, L. J. Hardwick, F. Bardé and P. G. Bruce, *Angewandte Chemie International Edition*, 2011, **50**, 8609-8613.
12. Z. Peng, S. A. Freunberger, Y. Chen and P. G. Bruce, *Science*, 2012, **337**, 563-566.
13. D. Kwabi, N. Ortiz-Vitoriano, S. Freunberger, Y. Chen, N. Imanishi, P. Bruce and Y. Shao-Horn, *MRS Bulletin*, 2014, **39**, 443-452.
14. Y.-C. Lu, Z. Xu, H. A. Gasteiger, S. Chen, K. Hamad-Schifferli and Y. Shao-Horn, *Journal of the American Chemical Society*, 2010, **132**, 12170-12171.
15. M. M. O. Thotiyl, S. A. Freunberger, Z. Peng, Y. Chen, Z. Liu and P. G. Bruce, *Nature materials*, 2013, **12**, 1050-1056.
16. B. Sun, X. Huang, S. Chen, P. R. Munroe and G. Wang, *Nano letters*, 2014, **14**, 3145-3152.
17. M. M. Ottakam Thotiyl, S. A. Freunberger, Z. Peng and P. G. Bruce, *Journal of the American Chemical Society*, 2012, **135**, 494-500.
18. J. Ming, W. J. Kwak, J. B. Park, C. D. Shin, J. Lu, L. Curtiss, K. Amine and Y. K. Sun, *ChemPhysChem*, 2014, **15**, 2070-2076.
19. S. Liu, Y. Zhu, J. Xie, Y. Huo, H. Y. Yang, T. Zhu, G. Cao, X. Zhao and S. Zhang, *Advanced Energy Materials*, 2014, **4**, n/a-n/a.
20. A. K. Thapa and T. Ishihara, *Journal of Power Sources*, 2011, **196**, 7016-7020.
21. F. Cheng and J. Chen, *Chemical Society Reviews*, 2012, **41**, 2172-2192.
22. Y. Chen, S. A. Freunberger, Z. Peng, O. Fontaine and P. G. Bruce, *Nature chemistry*, 2013, **5**, 489-494.
23. H. D. Lim, H. Song, J. Kim, H. Gwon, Y. Bae, K. Y. Park, J. Hong, H. Kim, T. Kim and Y. H. Kim, *Angewandte Chemie International Edition*, 2014, **53**, 3926-3931.
24. D. Sun, Y. Shen, W. Zhang, L. Yu, Z. Yi, W. Yin, D. Wang, Y. Huang, J. Wang and D. Wang, *Journal of the American Chemical Society*, 2014, **136**, 8941-8946.
25. W. Walker, V. Giordani, V. S. Bryantsev, J. Uddin, S. Zecevic, D. Addison and G. V. Chase, Meeting Abstracts, 2012.
26. T. H. Yoon and Y. J. Park, *RSC Advances*, 2014, **4**, 17434-17442.
27. L. Yang, J. T. Frith, N. Garcia-Araez and J. R. Owen, *Chem. Communications*, 2014.
28. B. J. Bergner, A. Schürmann, K. Peppler, A. Garsuch and J. r. Janek, *J Am Chem Soc*, 2014, **136**, 15054-15064.
29. G. V. Chase, S. Zecevic, W. T. Wesley, J. Uddin, K. A. Sasaki, G. P. Vincent, V. Bryantsev, M. Blanco and D. D. Addison, US Patent 20,120,028,137, 2012.
30. F. Pan, J. Yang, Q. Huang, X. Wang, H. Huang and Q. Wang, *Advanced Energy Materials*, 2014, **4**, n/a-n/a.
31. Q. Huang, H. Li, M. Gratzel and Q. Wang, *Physical Chemistry Chemical Physics*, 2013, **15**, 1793-1797.
32. Q. Wang, S. M. Zakeeruddin, D. Wang, I. Exnar and M. Grätzel, *Angewandte Chemie International Edition*, 2006, **45**, 8197-8200.
33. P. He, Y. Wang and H. Zhou, *Electrochemistry Communications*, 2010, **12**, 1686-1689.
34. Y. Wang, P. He and H. Zhou, *Advanced Energy Materials*, 2012, **2**, 770-779.
35. M. J. Lacey, J. T. Frith and J. R. Owen, *Electrochemistry Communications*, 2013, **26**, 74-76.
36. H. Ota, K. Shima, M. Ue and J.-i. Yamaki, *Electrochimica Acta*, 2004, **49**, 565-572.
37. L. El Ouatani, R. Dedryvere, C. Siret, P. Biensan, S. Reynaud, P. Iratcabal and D. Gonbeau, *Journal of the Electrochemical Society*, 2009, **156**, A103-A113.
38. S. Oswald, D. Mikhailova, F. Scheiba, P. Reichel, A. Fiedler and H. Ehrenberg, *Anal Bioanal Chem*, 2011, **400**, 691-696.
39. D. Ensling, M. Stjerndahl, A. Nytén, T. Gustafsson and J. O. Thomas, *Journal of Materials Chemistry*, 2009, **19**, 82-88.